JOURNAL OF BACTERIOLOGY, Apr. 2008, p. 3063–3075 Vol. 190, No. 8
0021-9193/08/$08.00+0 doi:10.1128/JB.01910-07

The Iron-Responsive Fur Regulon in *Yersinia pestis*▽‡

He Gao,[1,2]† Dongsheng Zhou,[2]† Yingli Li,[2]† Zhaobiao Guo,[2] Yanping Han,[2] Yajun Song,[2] Junhui Zhai,[2] Zongmin Du,[2] Xiaoyi Wang,[2] Jingmei Lu,[1]* and Ruifu Yang[2]*

College of Life Sciences, Northeast Normal University, Changchun 130024, People's Republic of China,[1] and State Key Laboratory of Pathogens and Biosecurity, Beijing Institute of Microbiology and Epidemiology, Beijing 100071, People's Republic of China[2]

Received 6 December 2007/Accepted 4 February 2008

The ferric uptake regulator (Fur) is a predominant bacterial regulator controlling the iron assimilation functions in response to iron availability. Our previous microarray analysis on *Yersinia pestis* defined the iron-Fur modulon. In the present work, we reannotated the iron assimilation genes in *Y. pestis*, and the resulting genes in complementation with those disclosed by microarray constituted a total of 34 genome loci (putative operons) that represent the potential iron-responsive targets of Fur. The subsequent real-time reverse transcription-PCR (RT-PCR) in conjunction with the primer extension analysis showed that 32 of them were regulated by Fur in response to iron starvation. A previously predicted Fur box sequence was then used to search against the promoter regions of the 34 operons; the homologue of the above box could be predicted in each promoter tested. The subsequent electrophoretic mobility shift assay (EMSA) demonstrated that a purified His_6 tag-fused Fur protein was able to bind in vitro to each of these promoter regions. Therefore, Fur is a global regulator, both an activator and a repressor, and directly controls not only almost all of the iron assimilation functions but also a variety of genes involved in various non-iron functions for governing a complex regulatory cascade in *Y. pestis*. In addition, real-time RT-PCR, primer extension, EMSA, and DNase I footprinting assay were used to elucidate the Fur regulation of the *ybt* locus encoding a virulence-required iron uptake system. By combining the published data on the YbtA regulation of *ybt*, we constructed a concise Fur/YbtA regulatory network with a map of the Fur-promoter DNA interactions within the *ybt* locus. The data presented here give us an overview of the iron-responsive Fur regulon in *Y. pestis*.

Iron acquisition is critical for the survival of pathogenic bacteria during infection. In mammals, iron is bound to Fe^{3+}-binding proteins (transferrin, lactoferrin, and ferritin) and hemopoteins (hemoglobin, haptoglobin-hemoglobin, hemopexin, and albumin, etc). The level of free iron (10 to 18 M) is too low to sustain bacterial growth (32). In light of the requirement for iron and the stiff competition for this nutrient, it is no surprise that successful pathogenic microorganisms have evolved miscellaneous strategies to scavenge iron from the iron or heme resources of mammalian hosts (1).

Bacteria regulate their iron metabolism in response to iron availability. An excess of cellular iron is toxic because of its ability to catalyze Fenton reactions leading to the formation of active species of oxygen. Iron uptake is, therefore, exquisitely regulated to maintain the intracellular concentration of this metal within desirable ranges. The predominant iron-regulating system in bacteria is the ferric uptake regulator (Fur) machinery (1, 13, 18). The Fur protein exhibits both sensory and regulatory functions in response to the intracellular iron concentration. Under iron-rich conditions, Fur binds to divalent ion, acquiring a configuration able to bind to target DNA sequences generally known as the Fur box, and inhibits the transcription of target genes/operons. Under iron-restricted conditions, Fur does not bind, and genes commonly responsible for iron assimilation functions are expressed, endowing bacterial cells with the ability to scavenge iron from various extracellular environments.

Plague, caused by *Yersinia pestis*, is one of the most dangerous diseases in the world. *Y. pestis* possesses an array of virulence determinants that promote infection in mammalian hosts and/or transmission by flea vectors (23, 34). A variety of iron acquisition systems (Ybt, Yfe, Yfu, Hmu, Has, Yiu, Iuc, and Fhu) have been characterized in *Y. pestis* (6, 7, 10, 15, 16, 20, 22, 25, 30), and at least two (Ybt and Yfe) of them were proven to be required for full virulence (6, 7). Thus, this bacterium has developed specialized strategies to obtain iron for its survival and growth in hosts during infection.

In our previous DNA microarray analysis (35), mRNA levels from wild-type (WT) *Y. pestis* cells treated with the iron chelator 2,2′-dipyridyl (DP) were compared to those supplemented with excessive iron, and then gene expression in the *fur* mutant was compared to that in the WT strain under iron-rich condition. This analysis identified genes both directly and indirectly controlled by Fur, leading to the defining of iron-Fur modulon that was defined as a collection of genes whose transcription was affected by both the DP treatment (the iron starvation) and the *fur* mutation.

In the present work, a total of 34 putative operons (mainly responsible for the iron assimilation functions) were identified as the direct Fur targets, based on the combined use of real-time reverse transcription-PCR (RT-PCR), primer extension analysis, and electrophoretic mobility shift assay (EMSA). It

* Corresponding authors. Mailing address for R. Yang: State Key Laboratory of Pathogens and Biosecurity, Beijing Institute of Microbiology and Epidemiology, Beijing 100071, People's Republic of China. Phone: (86) 10-66948594. Fax: (86) 10-63815689. E-mail: ruifuyang@gmail.com. Mailing address for J. Lu: College of Life Sciences, Northeast Normal University, Changchun 130024, People's Republic of China. E-mail: jingmlu@163.com.

† H.G., D.Z., and Y.L. contributed equally to this study.

‡ Supplemental material for this article may be found at http://jb.asm.org/.

▽ Published ahead of print on 15 February 2008.

was shown that Fur was a global regulator, both an activator and a repressor, governing a complex regulatory cascade in *Y. pestis*. The subsequent DNase I footprinting assay enabled the mapping of Fur-DNA interactions within the *ybt* locus, also known as the high pathogenicity island (HPI).

MATERIALS AND METHODS

Bacterial strains. The WT strain 201 was isolated from *Microtus brandti* in Inner Mongolia, China, with the phenotypes $F1^+$ (able to produce fraction 1 antigen or the capsule), VW^+ (presence of V antigen), Pst^+ (able to produce pesticin) and Pgm^+ (pigmentation on Congo red medium). It belongs to a newly established *Y. pestis* biovar, microtus (36), with a 50% lethal dose of <10 cells for mice by the subcutaneous challenge. The *fur* mutant (35) was constructed by using a Lambda Red recombination system (11).

Bacterial growth and RNA isolation. Both the WT and the *fur* mutant were grown at 26°C to mid-logarithmic phase (A_{620}, ~1.0) in a chemically defined TMH medium (29) containing 10 μM $FeCl_3$ as the sole iron source. The cell cultures were diluted by 20-fold in fresh TMH medium, and the cells experienced at least 10 generations in the medium at 26°C prior to reaching to an A_{620} of ~1.0. The cell cultures were then transferred to 37°C for 1 h. The culture was split, and one-half was treated with 100 μM DP to elicit the iron starvation. The other half was supplemented with an additional 40 μM $FeCl_3$ to ensure iron-rich conditions. Growth was continued for 30 min at 37°C, and then the cells were harvested to isolate total cellular RNA. RNA isolation was conducted as described previously (35).

Real-time RT-PCR. Gene-specific primers were designed to produce a 150- to 200-bp amplicon for each gene when *Y. pestis* genomic DNA was used as the template for PCR. The contaminated genomic DNA in RNA samples was removed by using an Ambion DNA-free kit. cDNA was generated by using 5 μg of total RNA and 3 μg of random hexamer primers. Real-time PCR was performed in triplicate for each RNA preparation by using LightCycler system (Roche) together with the Sybr green master mix, with a 1:200 dilution of cDNA as templates. To ensure that there was no contamination of genomic DNA, negative controls were performed by using "cDNA" generated without reverse transcriptase as templates. Reactions containing primer pairs without template were also included as blank controls. A standard curve was made for each RNA preparation with the 16S rRNA gene. Relative transcriptional level was determined by calculating the threshold cycle (ΔC_T) of each gene. The 16S rRNA gene was used to normalize all of the other genes. The transcriptional variation for each gene in relative quantity of cDNA molecules present under the indicated paired conditions was ultimately calculated. A mean ratio of two was taken as the cutoff of statistical significance.

Primer extension. Primer extension assay was performed by using a primer extension system-AMV reverse transcriptase kit (Promega). The extension primers were end labeled with [γ-^{32}P]ATP. Three nanograms of each end-labeled primer were annealed with 10 to 30 μg of total RNA and extended according to the manufacturer's protocol. cDNA products were recovered by ethanol precipitation and subjected to electrophoresis in a 6% polyacrylamide–8 M urea gel. The gel was analyzed by autoradiography (Kodak film). To serve as sequence ladders, sequencing reactions were also performed with the same primers used for primer extension, using an fmol DNA cycle sequencing system (Promega).

Preparation of His-Fur and Fur with the His tag removed. The entire *fur* coding region of strain 201 was cloned into plasmid pET28a (Novagen) (between BamHI and HindIII sites). The recombinant plasmids encoding a His-Fur fusion protein were transformed into *Escherichia coli* BL21(DE3) cells. Overexpression of His-Fur was induced by addition of isopropyl-β-D-thiogalactoside. The recombinant His-Fur protein was purified under native conditions with a QIAexpressionist Ni^{2+}-affinity column (Qiagen), since its His tag is able to bind to the Ni^{2+} molecule in the column. After we stringently washed off contaminated proteins, we eluted the purified His-Fur protein with the elution buffer (250 mM iminazole, 50 mM NaH_2PO_4, 300 mM NaCl).

To cleave the His tag, the thrombin (Novagen, Madison, WI) was incubated with the uneluted, purified His-Fur (after the above stringent washing) in a Ni-nitrilotriacetic acid column at 4°C for 14 h. The subsequent washing and elution were conducted as described above. The eluted liquids were collected sequentially into various tubes, each at a volume of 500 μl, and then the protein sample in each tube was subjected to sodium dodecyl sulfate–15% polyacrylamide gel electrophoresis (SDS–15% PAGE). The thrombin-cleaved Fur (TC-Fur) protein would be present in the former several tubes according to SDS-PAGE, given that this protein still has 11 His residues scattered in its protein sequence (it thereby is able to bind to the Ni^{2+} column, with an affinity lower than that of His-Fur).

The eluted, purified His-Fur or TC-Fur was dialyzed and then concentrated to a final concentration of 0.1 to 0.3 mg/ml in the storage buffer containing Tris-HCl (pH 7.5), 50 mM NaCl, 2 mM $CaCl_2$, and 15% glycerol by using an Amicon Ultra-15 (Millipore). The purity of the resulting His-Fur–TC-Fur was verified by SDS–15% PAGE.

EMSA. Primers were designed to amplify the 400- to 500-bp promoter-proximate region extending upstream from the start codon of each first gene of the operons tested. An EMSA was performed by using the gel shift assay system (Promega). The 5′ ends of DNA were labeled by using [γ-^{32}P]ATP and T4 polynucleotide kinase. DNA binding was performed in a 10-μl reaction volume containing binding buffer (100 μM $MnCl_2$, 1 mM $MgCl_2$, 0.5 mM dithiothreitol, 50 mM KCl, 10 mM Tris-HCl [pH 7.5], 0.05 mg of sheared salmon sperm DNA/ml, 0.05 mg of bovine serum albumin/ml, and 4% glycerol), labeled DNA (1,000 to 2,000 cpm/μl), and increasing amounts of His-Fur or Fur with the His tag removed. We still included two control reactions: one contained the specific DNA competitor (unlabeled promoter DNA regions), while the other is the nonspecific protein competitor (rabbit anti-F1-protein polyclonal antibody). After incubation at room temperature for 30 min, the products were loaded onto a native 4% (wt/vol) polyacrylamide gel and electrophoresed in 0.5× Tris-borate (TB) buffer containing 100 μM $MnCl_2$ for 30 min at 220 V. Radioactive species were detected by autoradiography.

DNase I footprinting. To obtain each promoter DNA fragment with a single ^{32}P-labeled end, PCR amplification was performed with the promoter-specific primer pair used in the EMSA, except that either the sense or the antisense primer was end labeled. The PCR products were purified by using MinElute reaction cleanup columns (Qiagen). Increasing amounts of His-Fur was incubated with the purified, labeled DNA fragment (2 to 5 pmol) for 30 min at room temperature in a final 10-μl reaction volume containing the same binding buffer used for the EMSA. Before DNA digestion, 10 μl of Ca^{2+}/Mg^{2+} solution (5 mM $CaCl_2$ and 10 mM $MgCl_2$) was added, followed by the incubation for 1 min at room temperature. Then, the optimized RQ1 RNase-Free DNase I (Promega) was added to the reaction mixture, and the mixture was incubated at room temperature for 40 to 90 s. The reaction was quenched by adding 9 μl of the stop solution (200 mM NaCl, 30 mM EDTA, and 1% SDS), followed by incubation for 1 min at room temperature. The partially digested DNA samples were extracted with phenol-chloroform, precipitated with ethanol, and analyzed in a 6% polyacrylamide–8 M urea gel. Protected regions were identified by comparison with the sequence ladders. For sequencing, we used the fmol DNA cycle sequencing system (Promega). The templates for sequencing were the same as the DNA fragments of DNase I footprinting assays. Radioactive species were detected as described above.

Computational promoter analysis. The 500-bp promoter region extending upstream from the start codon of every first gene in each indicated operon was retrieved with the retrieve-seq program (31). Matching the Fur consensus sequence within the promoter regions was performed by using the patser-matrix tool (31). This analysis generated a weight score for each promoter DNA. A larger number of this score value corresponds to a higher probability of the presence of a Fur site.

RESULTS AND DISCUSSION

Collection of candidate genes. In addition to the characterized iron acquisition systems (Ybt, Yfe, Yfu, Hmu, Has, Yfu, Yiu, Iuc, and Fhu), there are still several other predicted iron assimilation (acquisition and/or storage) functions in the genome annotation of *Y. pestis* CO92 (27), KIM (33), and 91001 (28). To give a full collection of iron assimilation systems in *Y. pestis*, all available literatures about bacterial iron assimilation were reviewed, and the deriving protein sequences of reported bacterial iron assimilation genes were compared to the genomic sequence data of CO92, by using the BLASTP, to find their homologues in *Y. pestis*. In addition, the BLASTP analysis of all of the iron-Fur modulon members of *Y. pestis*, as determined by our previous microarray expression analysis (35), was performed against the GenBank data to test whether each of them was homologous to a bacterial iron assimilation gene. Taken together, a total of 20 proven or putative iron assimi-

lation-related genomic loci (80 genes) were found in *Y. pestis*, as shown in Table 1.

Beside the above iron assimilation genes, Table 1 still included the following genes: (i) genes whose transcription was affected by both DP treatment and the *fur* mutation, as shown by our previous microarray analysis (35) (these genes encode various non-iron functions), and (ii) several genes belonging to the iron uptake-associated gene cluster, as determined by the clustering analysis on the data of 25 microarray expression profiles of *Y. pestis* (in addition, EMSA has shown that the His-Fur binds to the upstream DNA region of these genes) (17).

All of the genes in Table 1 were visually scrutinized according to the transcriptional organization in relation to their surrounding genes to identify the putative operons (defined as a cluster of adjacent genes that have intergenic regions <150 bp in length and were putatively or definitely transcribed in the same orientation). This analysis generated a total of 34 operons, and 13 of them contained only a single gene.

Identification of iron-responsive Fur-regulated genes. For every first gene in each of the above 34 operons, the real-time RT-PCR analysis was performed so that the mRNA level from WT cells treated with DP was compared to those supplemented with excessive iron, and then gene expression in the *fur* mutant was compared to that in the WT strain under iron-rich conditions. It was found that, except for *fepB* (YPO0701) and *fcuA* (YPO1753), the transcription of all of the other genes tested was shown to be affected by both the DP treatment and the *fur* mutation.

Both *fepB* and *fcuA* encoded the iron acquisition function. The primer extension assay further confirmed that their transcription was independent of both Fur and iron (Fig. 1). For the primer extension assay, we used the same RNA preparations to analyze the Fur- and iron-dependent transcription of each gene tested. An oligonucleotide primer was designed to be complementary to a portion of the RNA transcript of each gene (operon). The yield of each primer extension product would indicate the mRNA level of the corresponding gene (operon) under the specific growth condition.

Both the previous microarray analysis (35) and the current RT-PCR assay were conducted by using the same *Y. pestis* strains and identical growth conditions. However, the comparison between these two kinds of data revealed the discrepancy for 10 operons, i.e., the negative results in microarray compared to RT-PCR (Table 1). The further primer extension assay on eight of these operons showed the reasonability of the RT-PCR data (see Fig. 1 and 3). DNA microarray offers a powerful tool for genomewide analysis of gene regulation at the transcriptional level, enabling the identification of both regulons and stimulons (37). However, its result is influenced by microarray construction, RNA extraction, probe labeling, hybridization conditions, and data analysis (21, 26, 37). Because of the inherent limitations in reliability, microarray results should be validated by at least one traditional method (37).

Along with our previous microarray data, the real-time RT-PCR analysis in conjunction with the primer extension assay herein enabled the identification of a large array of genes or operons whose transcription was regulated, both positively and negatively, by Fur using the iron as the cofactor. Expect for *fepB* and *fcuA* genes, all of the other proven or predicted iron acquisition systems in *Y. pestis* should be induced in response to the iron starvation, which is mediated by the transcriptional repression of Fur protein using the iron as corepressor.

Like other bacteria, *Y. pestis* possesses two types of iron storage functions, the Bfr-Bfd system (the haem-containing bacterioferritin and the Bfr-associated ferredoxin, respectively) and FtnA (the haem-free ferritin) (19). The iron-Fur complex divergently modulated the transcription of these two iron-storage functions (Table 1).

The iron-Fur complex still affected some genes involved in various non-iron functions (ribonucleoside-diphosphate reductase, Fe-S cluster assembly, electron transport, and oxidative defense, etc.) and also a variety of genes with unknown function. In addition to its classically negative regulatory activities, Fur activates gene transcription, indicating that Fur is a global regulator rather than a specific repressor.

Computational analysis of Fur sites. The *E. coli* Fur protein, upon association with iron, binds a 19-bp consensus site with the sequence 5′-GATAATGATAATCATTATC-3′ (known as the classic Fur box) and represses the transcription of downstream gene (13). Based on our previous microarray data, the regulatory motif discovery analysis generated a conserved motif, which was considered as the Fur consensus in *Y. pestis* (35). A concise interpretation of this consensus showed a 9-1-9 inverted repeat (5′-AATGATAATNATTATCATT-3′). In addition, a position frequency matrix (PFM) that represented the conserved signals for Fur recognition in *Y. pestis* was subsequently obtained (see supplemental data S1 for details).

The 500-bp upstream DNA region of every first gene in each of the 34 operons listed in Table 1 (including *fepB* and *fcuA*) was screened with the above PFM. Its homologue could be predicted in each promoter sequence analyzed. The presence of a sequence with high similarity with Fur consensus is a very good predictor of Fur-specific binding.

Characterization of recombinant His-Fur and Fur. A recombinant His-Fur protein was expressed in *E. coli* by using the pET28a vector. A 34-amino-acid peptide including a His_6 tag was fused with Fur at its N terminus. The His tag was subsequently cleaved by thrombin. Compared to the WT Fur protein of *Y. pestis*, the TC-Fur (thrombin-cleaved Fur) still contained 17 amino acid resides at its N terminus. As expected, the size of TC-Fur is slightly less than that of His-Fur, as verified by SDS–15% PAGE (see Fig. S1 in supplemental data S2).

We further characterized the DNA-binding properties of His-Fur/TC-Fur by using EMSA. For EMSA, the primers were designed to amplify a 400- to 500-bp DNA fragment upstream from the translational start site for each gene tested. Each upstream promoter DNA is radioactively labeled, incubated with a purified His-Fur or TC-Fur protein, and then subjected to native gel electrophoresis. It has been shown previously in other bacteria that the binding affinity of Fur to regulatory DNA sequences is dependent on the presence of divalent metal ions and that the addition of EDTA will result in a loss of affinity of Fur (12, 13). The Mn^{2+} ions are routinely used in the Fur-binding experiments in place of Fe^{2+} because of its greater redox stability (12, 13). Accordingly, we tested different modified binding/electrophoresis buffers by EMSA (by removing Mn^{2+} and/or EDTA in each buffer), using the *ybtP* pro-

TABLE 1. Iron-responsive Fur regulon in *Y. pestis*[a]

Function	Microarray		RT-PCR		Primer extension[b]		Gel shift	Predicted Fur site		Gene[c]	Gene	Product
	DP	*fur*	DP	*fur*	DP	*fur*		Position[d]	Sequence[e]			
Iron acquisition system: Fe^{2+} transporter Feo	2.02	2.99	2.25	4.11			+	R/–115/9.9	ACTGAGAATTA TTTTCATG	YPO0132 ↑ YPO0133 ↑	*feoB* *feoA*	Ferrous iron transport protein B Ferrous iron transport protein A
Iron acquisition systems: ABC-type iron transporters	2.84	12.49	2.26	4.83			+	D/–36/16.13	ATTGATAATCA TTTTCATT	YPO2439 ↓ YPO2440 YPO2441 YPO2442	*yfeA* *yfeB* *yfeC* *yfeD*	Iron ABC transporter, periplasmic binding protein Iron ABC transporter, ATPase component Iron ABC transporter, permease component Iron ABC transporter, permease component
	5.89	6.35	11.03	17.46			+	D/–105/14.74	AATGATAATCA TTTTTATT	YPO2958 ↓ YPO2959 YPO2960	*yfuA* *yfuB* *yfuC*	Iron ABC transporter, periplasmic binding protein Iron ABC transporter, permease component Iron ABC transporter, ATPase component
Iron acquisition systems: siderophore-based	**1.10**	**1.02**	4.68	3.93	Verified	Verified	+	D/–176/7.0	AACGATAAGA ATTCTTAAT	YPO0164 ↑		Putative ferric siderophore receptor protein
	–1.15	**–1.12**	**1.04**	**1.21**	Verified*	Verified*	+	R/–226/8.14	AATAATAGTAA TGAACATC	YPO0701 ↑	*fepB*	Putative ferric enterobactin (enterochelin) binding protein
										YPO0770 ↑		Putative siderophore ABC transporter, permease component
										YPO0771		Putative siderophore ABC transporter, permease component
										YPO0772		Putative signal transducer
										YPO0773		Putative thioesterase
										YPO0774		Putative siderophore biosysnthesis protein
										YPO0775		Putative siderophore biosysnthesis protein
										YPO0776		Putative siderophore biosysnthesis protein
										YPO0777		Putative siderophore biosysnthesis protein
							-			YPO0778		Putative siderophore biosysnthesis protein
										YPO1012		Putative peptide/polyketide synthase subunit
	6.92	49.65	6.77	16.38			+	D/–184/13.37	AATGATAATCG TTTGCAAT	YPO1011		Putative TonB-dependent outer membrane siderophore receptor
	1.01	**1.02**	2.43	3.09	ND	ND	+	R/–176/11.7	AATGATAATCA AAATCGTT	YPO0955 ↓ YPO0956		H YPOthetical protein Putative hydroxamate-type ferric siderophore receptor
	2.83	8.68	2.39	2.43			+	R/–66/14.42	AGTGGTTATCA TTATCAAT	YPO0989 ↓	*iucA*	Putative aerobactin biosynthesis protein IucA (pseudogene)
										YPO0991	*iucB*	Putative aerobactin biosynthesis protein IucB
										YPO0992	*iucC*	Putative aerobactin biosynthesis protein IucC
										YPO0993	*iucD*	Putative aerobactin biosynthesis protein IucD
										YPO0994	*iutA*	Putative aerobactin receptor

104.56	15.69	3.55	5.57			+	D/–66/12.88	ATTGATAAGTA TTATCATT	YPO1310	*yiuA*	Putative siderophore ABC transporter, periplasmic binding protein
									YPO1311	*yiuB*	Putative siderophore ABC transporter, permease component
									YPO1312	*yiuC*	Putative siderophore ABC transporter, ATPase component
									YPO1313	*yiuR*	Putative outer membrane siderophore receptor
8.90	8.59	3.63	4.22			+	D/–64/15.28	ATTGATAATCA CTATCATT	YPO1528	*ysuF*	Putative ferric iron reductase
									YPO1529	*ysuJ*	Putative decarboxylase
									YPO1530	*ysuI*	Putative siderophore biosynthetic enzyme
									YPO1531	*ysuH*	Putative siderophore biosynthetic enzyme
									YPO1532	*ysuG*	Putative siderophore biosynthetic enzyme
									YPO1533	*ysuD*	Putative siderophore ABC transporter, ATPase component
									YPO1534	*ysuC*	Putative siderophore ABC transporter, permease component
									YPO1535	*ysuB*	Putative siderophore ABC transporter, permease component
									YPO1536	*ysuA*	Putative siderophore ABC transporter, periplasmic binding protein
									YPO1537	*ysuR*	Putative outer membrane siderophore receptor
1.72	2.34	4.37	2.03	Verified	Verified	+	D/–202/14.49	AATAATAATCA TTTGCATT	YPO1538	*ysuE*	Putative siderophore biosynthetic enzyme
MD	**MD**	**1.47**	**0.99**	Verified*	Verified*	+	R/–61/5.79	AATGCTTATCA TAAGGATT	YPO1753	*fcuA*	Ferrichrome receptor protein
12.68	2.48	2.34	2.45			+	D/–71/14	AATAGTTATCA TTTTCAAT	YPO1906	*fyuA*	Pesticin/yersiniabactin receptor protein
									YPO1907	*ybtE*	Yersiniabactin biosynthetic protein
									YPO1908	*ybtT*	Yersiniabactin biosynthetic protein
									YPO1909	*ybtU*	Yersiniabactin biosynthetic protein
									YPO1910	*irp1*	Yersiniabactin biosynthetic protein
4.19	**–1.07**	3.56	2.75	Verified	Verified	+	R/–66/13.87	AATAATAATTA TTAACAAT	YPO1911	*irp2*	Yersiniabactin biosynthetic protein
8.63	**–1.07**	3.86	2.25	Verified	Verified	+	D/–87/14.52	AATAATAACCA TTATCAAT	YPO1912	*ybtA*	Transcriptional regulator YbtA
8.48	**–1.08**	5.20	2.87	Verified	Verified	+	R/–98/14.52	AATAATAACCA TTATCAAT	YPO1913	*ybtP*	Yersiniabactin ABC transporter, permease and ATPase components
									YPO1914	*ybtQ*	Yersiniabactin ABC transporter, permease and ATPase components
									YPO1915	*ybtX*	Putative signal transducer
									YPO1916	*ybtS*	Salicylate synthetase
40.24	74.24	2.64	2.56			+	D/–100/13.22	AATGATAATTG ATATCATT	YPO3340		Putative ferric siderophore receptor (pseudogene)

Continued on following page

TABLE 1—*Continued*

Function	Microarray		RT-PCR		Primer extension[b]		Gel shift	Predicted Fur site		Gene[c]	Gene	Product
	DP	*fur*	DP	*fur*	DP	*fur*		Position[d]	Sequence[e]			
										YPO3390	*fhuB*	Putative ferrichrome ABC transporter, permease component
										YPO3391	*fhuD*	Putative ferrichrome ABC transporter, periplasmic binding protein
	1.43	**1.15**	MD	MD	Verified	Verified	+	R/–177/8.91	AATAATTATCA AAACCGTT	YPO3392	*fhuC*	Putative ferrichrome ABC transporter, ATPase component
	4.28	2.96	2.19	2.24			+	D/–59/13.02	AATAAAAATCA TTAGCATT	YPO4022	*fitA*	Putative siderophore ABC transporter, periplasmic binding protein
										YPO4023	*fitB*	Putative siderophore ABC transporter, permease component
										YPO4024	*fitC*	Putative siderophore ABC transporter, permease component
										YPO4025	*fitD*	Putative siderophore ABC transporter, ATPase component
Iron acquisition system: hemopore-based										YPO3918	*hasB*	Has-sepcific TonB homolog
										YPO3919	*hasE*	Hemophore ABC-exporter, permease component
										YPO3920	*hasD*	Hemophore ABC-exporter, ATPase component
										YPO3922	*hasA*	Hemophore HasA
	MD	**1.45**	2.01	2.15	ND	ND	+	R/–343/14	AATGATTATCA TAATCACT	YPO3923	*hasR*	TonB-dependent outer membrane hemophore receptor
Iron acquisition system: heme/hemoglobin receptor-based										YPO0279	*hmuV*	Hemin ABC transporter, ATPase component
										YPO0280	*hmuU*	Hemin ABC transporter, permease component
										YPO0281	*hmuT*	Hemin ABC transporter, periplasmic binding protein
										YPO0282	*hmuS*	Cytoplasmic hemin-degrading proteinon
	5.22	8.34	5.83	10.68			+	D/–362/11.94	ACTGATAGTCG TTATCATT	YPO0283	*hmuR*	TonB-dependent outer membrane hemin receptor
TonB-ExbB-ExbD complex: providing energy for iron acquisition	4.39	6.79	3.82	2.17			+	D/–416/15.21	AATGATAATTA CTATCAAT	YPO0682	*exbB*	ExbB protein
										YPO0683	*exbD*	ExbD protein
	2.49	2.90	2.07	2.45			+	D/–281/10.46	AATAATGATAG TTATCAAT	YPO2193	*tonB*	TonB protein
Iron storage	2.50	2.83	16.72	15.15			+	D/–55/9.03	AATAAAACTCA TTCTTATT	YPO0205	*bfd*	Bacterioferritin-associated ferredoxin
										YPO0206	*bfr*	Bacterioferritin
	–5.21	–4.41	–10.07	–20.31			+	R/–201/12.97	CATGATAATCA TTCACATT	YPO1783	*ftnA*	Ferritin

Fur-repressed various/ unknown functions	4.98	14.11	4.91	7.45			+	R/–88/15.07	AATGATAATCA TAACCAAT	YPO0426 ↓		Membrane protein
	3.92	5.94	2.27	2.46			+	D/–92/14.42	AGTGGTTATCA TTATCAAT	YPO0988 ↑		Membrane protein
	8.90	8.59	3.63	4.22			+	D/–64/15.28	ATTGATAATCA CTATCATT	YPO1528 ↓		Ferric iron reductase
										YPO1529 ↓		Decarboxylase
	2.22	2.14	2.16	2.63			+	R/–27/9.21	CCTGATAACGA TTTTCATT	YPO2163 ↓		Nitroreductase
										YPO2399 ↑	*sufE*	Sulfur acceptor protein
										YPO2400	*sufS*	Selenocysteine lyase, PLP-dependent
										YPO2401	*sufD*	Component of SufBCD complex
										YPO2402	*sufC*	Component of SufBCD complex, ATP-binding component of ABC superfamily
										YPO2403	*sufB*	Component of SufBCD complex
	3.24	**1.82**	3.17	2.44	Verified	Verified	+	D/–153/13.61	AGTGATAATTA TTATCACT	YPO2404	*sufA*	Fe-S cluster assembly protein
										YPO2648 ↑	*nrdF*	Ribonucleoside-diphosphate reductase 2 beta chain
										YPO2649	*nrdE*	Ribonucleoside-diphosphate reductase 2 alpha chain
										YPO2650	*nrdI*	NrdI protein homologue
	5828.29	5.59	4.77	10.51			+	D/–94/6.12	GATGATAATCA TAGGCCAC	YPO2651	*nrdH*	Glutaredoxin
	2.07	MD	8.01	14.51			+	D/–75/12.88	CTTGATAATTA TTCTCATT	YPO2982 ↑	*mntH*	Manganese transport protein MntH
Fur-activated non-iron functions	–2.65	–5.16	–2.32	–5.52			+	D/–230/8.6	AATGATCATAA TTTCAAAT	YPO1207 ↑	*katA*	Catalase
										YPO3036 ↑	*napC*	Cytochrome C-type protein NapC
										YPO3037	*napB*	Cytochrome C-type protein NapB precursor
										YPO3038	*napA*	Periplasmic nitrate reductase precursor
										YPO3039	*napD*	Conserved h YPOthetical protein
	–5.42	–5.69	–2.64	–2.33			+	D/–102/14.2	AATAAGAATTA TTATCATT	YPO3040	*napF*	Ferredoxin-type protein NapF

[a] For DP, the RNA from WT cells treated with 100 μM DP was compared to that with the addition of 40 μM $FeCl_3$. For *fur*, the mRNA expression in the *fur* mutant was compared to that in the WT strain grown under iron-rich conditions. The numerical data for DP and *fur* are presented as the mean change of mRNA level for each gene under the paired growth conditions. A positive number represents the fold increase, while a minus sign indicates a fold decrease. Data for nondifferentially regulated genes and those with missing data (MD) are indicated in boldface type. The microarray results have been published previously (35).

[b] The term "Verified" indicates that there was the discrepancy between the data determined by RT-PCR and microarray (a total of ten operons); for eight of them the subsequent primer extension assay verified the rationality of the RT-PCR results. ND, not determined. *, RT-PCR and/or microarray indicated that the transcription of the corresponding genes was independent of both Fur and iron; this was further confirmed by the primer extension assay.

[c] The gene identification numbers were derived from the genome annotation of *Y. pestis* CO92. Putative operons (35 in all) are boxed, and vertical arrows indicate the transcriptional organization. The genes YPO1011-1012 and YPO0778-0770 are harbored in a continuous genomic region in KIM and 91001, encoding a putative siderophore-based iron acquisition system. This genomic region splits into two separate genomic loci (YPO1011-1012 and YPO0778-0770) in CO92, probably due to the IS sequence-base homologous recombination. Thus, YPO1011-1012 and YPO0778-0770 was considered to be a single putative operon in *Y. pestis*. As expected, the EMSA showed that His-Fur bonds to the upstream DNA region of YPO1011, the first gene of the above siderophore-based system, rather than that of YPO0778 (see also Fig. 2) that was actually an internal member of this system.

[d] The strand/distance of the Fur site upstream of transcriptional start site/matching score are indicated.

[e] Matching the predicted *Y. pestis* Fur box within the 500-bp promoter regions was performed by using the program patser-matrix (see the text). The most strongly matched Fur site was indicated with a weight score for each promoter DNA.

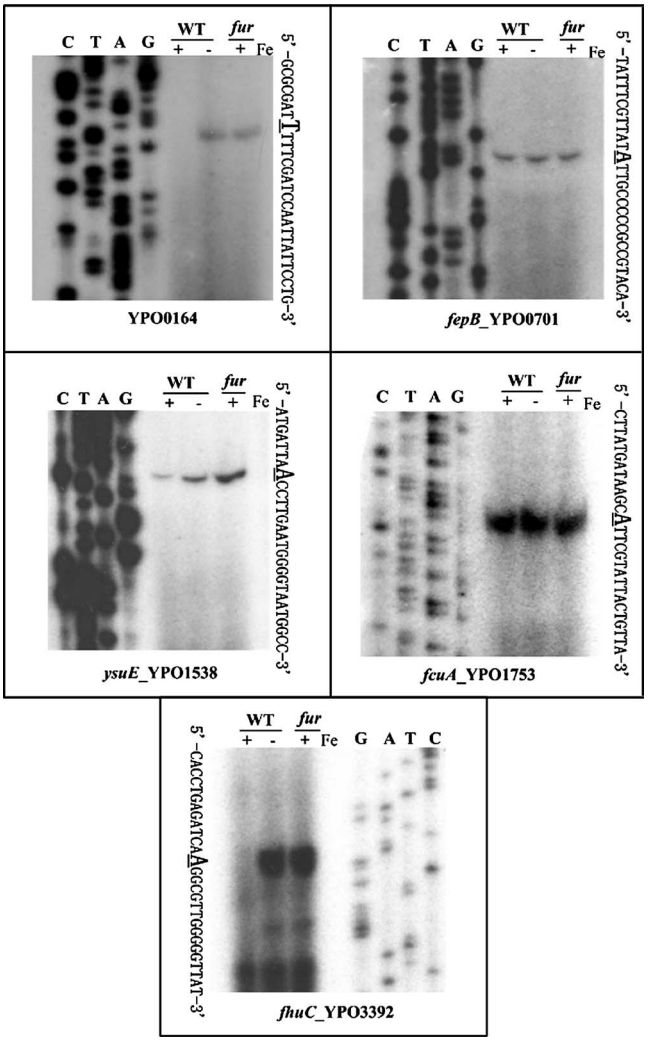

FIG. 1. Primer extension analysis of five selected genes. There were 10 operons for which the RT-PCR data were inconsistent with the microarray ones (see Table 1). Five (YPO0164, *fepB*, *ysuE*, *fcuA*, and *fhuC*) of them were chosen for primer extension analysis. RNA was isolated from the WT strain or the *fur* mutant grown in the presence (−) or absence (+) of iron. By using an oligonucleotide primer complementary to RNA transcript, cDNA was synthesized from the RNA templates. Electrophoresis of primer extension products was performed with a 6% polyacrylamide–8 M urea gel. Lanes C, T, A, and G represent the Sanger sequencing reactions. The transcriptional start sites were underlined.

moter region as the DNA probe (see Fig. S2 in supplemental data S2). It was demonstrated that the presence of Mn^{2+} (100 μM) plus the absence of EDTA in both binding and electrophoresis buffers would give the strongest binding affinity of His-Fur–TC-Fur. Accordingly, buffers containing 100 μM Mn^{2+} without EDTA would be used for the following DNA-binding experiments.

In addition, the promoter regions of four genes (*yptP*, YPO2163, *bfd*, and *yfeA*) were analyzed by EMSA to compare the DNA-binding affinities of His-Fur–TC-Fur (see Fig. S3 in supplemental data S2). The results showed that the TC-Fur protein had a DNA binding affinity stronger than that of His-Fur.

To compare the DNA-binding sites of His-Fur–TC-Fur, the DNase I footprinting assay was performed on both coding and noncoding strands of PCR-generated *ybtP* promoter fragment (see Fig. S4 in supplemental data S2). The radioactively labeled promoter DNA was incubated with increasing amounts of His-Fur or TC-Fur; after partial digestion with DNase I, the resulting fragments were analyzed by denaturing gel electrophoresis. Both His-Fur and TC-Fur gave an identical footprint (an identical binding site) on each DNA strand.

Taken together, the DNA binding properties of His-Fur were almost identical to those of TC-Fur. Accordingly, the His-Fur protein was used in the following EMSA and DNase I footprinting experiments, since it was more convenient to be purified.

Investigation of Fur-recognized promoters by EMSA. The mere presence of a Fur consensus sequence, as detected by the above computational promoter analysis, does not necessarily mean that Fur should bind to these DNA sites. Accordingly, the upstream DNA region of every first gene of each of the 34 operons in Table 1 was investigated by using EMSA to determine whether Fur would bind to these promoter regions in vitro. It was shown that the His-Fur protein was able to bind in vitro to each of the upstream DNA regions described above (Fig. 2).

To confirm the specificity of EMSA, the EMSA experiments still included the 269- and 528-bp DNA fragments in the coding regions of 16S rRNA and *ybtP* genes, respectively, as well as a 456-bp upstream DNA fragment of YPO0778, as the negative controls (Fig. 2). The genes YPO1011-1012 and YPO0778-0770 were located in a continuous genomic region in KIM, encoding a putative siderophore-based iron acquisition system. Interestingly, this genomic region splits into two separate genomic loci (YPO1011-1012 and YPO0778-0770) in CO92 due to the IS sequence-based homologous recombination. As expected, the EMSA showed that Fur bound to the upstream DNA region of YPO1011, the first gene of the siderophore-based system described above, rather than that of YPO0778 (Fig. 2), an internal member of this system. The *ybtP* gene is the first gene of the *YbtPQXS* operon in the HPI, and EMSA showed that His-Fur recognized the upstream promoter region of this gene. Here, it was shown by EMSA that His-Fur did not bind to the coding regions of both 16S rRNA and *ybtP* genes (Fig. 2).

Accordingly, the EMSA experiments demonstrated that the Fur protein could recognize in vitro the promoter sequences of all of the operons listed in Table 1. We concluded that the operons giving a positive result in both EMSA and RT-PCR experiments were the direct targets of Fur using the iron as the cofactor. All of these genes or operons constituted the iron-responsive Fur regulon in *Y. pestis*.

The transcription of *fepB* and *fcuA* was independent of both Fur and iron, as determined by microarray, RT-PCR and primer extension. It should be noted that the result described above is confined to *Y. pestis* strain 201 under the growth conditions presented here. However, both computational promoter analysis and EMSA showed that Fur recognized the promoters of these two genes. Given that both of them encoded the iron acquisition functions, we presumed that the transcription of these two genes should be under the direct control of Fur (so they were still included in Table 1). Further

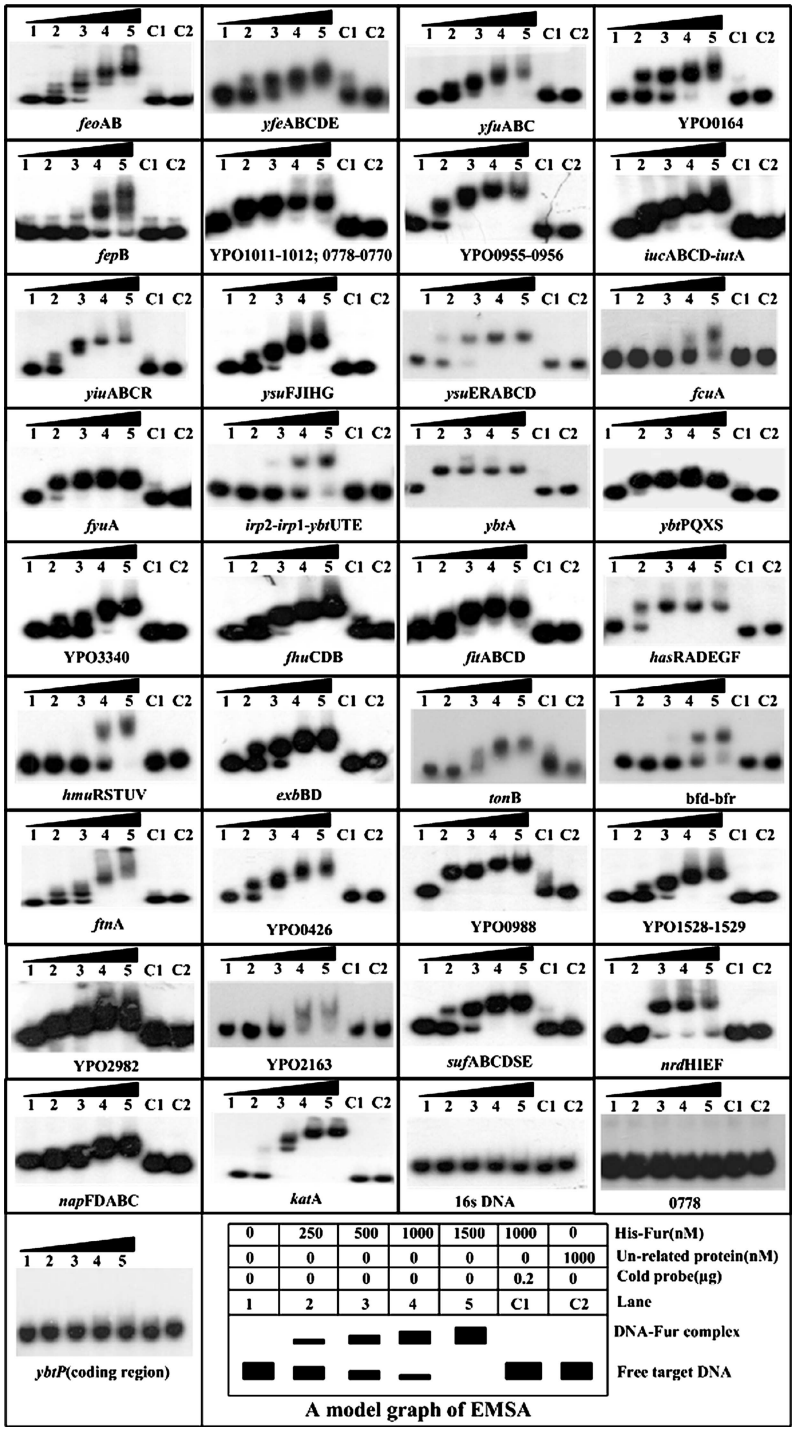

FIG. 2. EMSAs. The PCR-generated, [γ-^{32}P]-labeled target DNA probe or the corresponding cold probe (i.e., unlabeled target DNA) was incubated with the purified His-Fur protein or an unrelated protein (purified goat anti-rabbit anti-F1 antigen antibody). The mixtures were directly subjected to the 4% (wt/vol) PAGE. The band of free promoter DNA disappears with increasing amount of Fur protein, and a retarded DNA band with decreased mobility turns up, which presumably represents the Fur-DNA complex. A model graph of EMSA is shown as well.

experiments on the typical virulent *Y. pestis* strains and/or other appropriate growth conditions are needed to elucidate it.

Fur-DNA interactions within HPI. The *pgm* locus is a 102-kb unstable DNA region (YPO1902–1967 on the chromosome of CO92) embedded between two IS*100* elements in the same orientation (8). The recombination between the two IS*100* elements will delete this locus. YPO1902–, containing the *ybt* locus, was referred to as the HPI. Mutants lacking the Ybt system (a well-characterized siderophore-based iron acquisition system) are completely avirulent to mice by subcutaneous infection but are

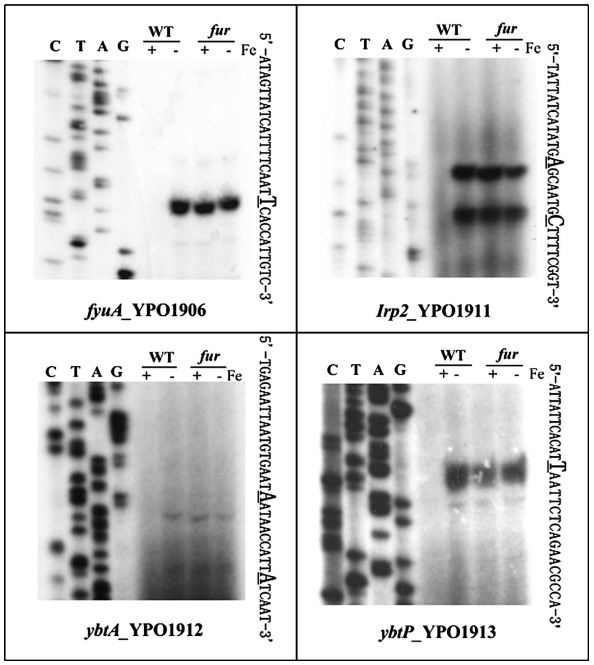

FIG. 3. Primer extension analyses of the HPI genes. Primer extensions assay was carried out to determine the transcriptional start sites of *fyuA*, *irp2*, *ybtA*, and *ybtP*. See Fig. 1 for the technical notes. *irp2*, *ybtA*, and *ybtP* also belonged to the 10 operons whose RT-PCR data were inconsistent with their microarray ones (Table 1).

fully virulent via an intravenous route (7), suggesting that the Ybt is essential to iron acquisition at the site of flea bite, in the lymphatic system and/or the lymph nodes.

The *ybt* locus is transcribed into four operons (*fyuA*, *irp2-irp1-ybtUTE*, *ybtA*, and *ybtPQXS*) (9, 10). RT-PCR analysis here showed that the whole *ybt* locus was induced in response to iron starvation, which is mediated by the transcriptional repression of Fur protein using iron as corepressor. In addition to confirmation of the RT-PCR results presented above, the primer extension was used to map the 5′ terminus of RNA transcript of each of these four operons, enabling the determination of transcriptional start sites and helping to localize the core promoter region (−10 and −35 elements). The length of detecting cDNA reflects the number of bases between the labeled nucleotide of the primer and the 5′ end of RNA transcript. A single transcriptional start site (a single primer extension product) was detected for each of *fyuA* and *ybtPQXS* (Fig. 3). Thus, a single promoter was transcribed for each operon under the iron starvation condition. Two transcriptional start sites (two primer extension products) were detected for *irp2-irp1-ybtUTE* and *ybtA*, indicating that two promoters were transcribed for each operon (Fig. 3). All of the detecting promoters here were repressed by the Fur regulator upon the extracellular iron excess.

Then, the DNase I footprinting assay was used to identify the precise Fur sites within the Fur-dependent promoters discussed above. This analysis confirmed the binding of His-Fur protein to these promoter DNA samples, as seen in EMSA.

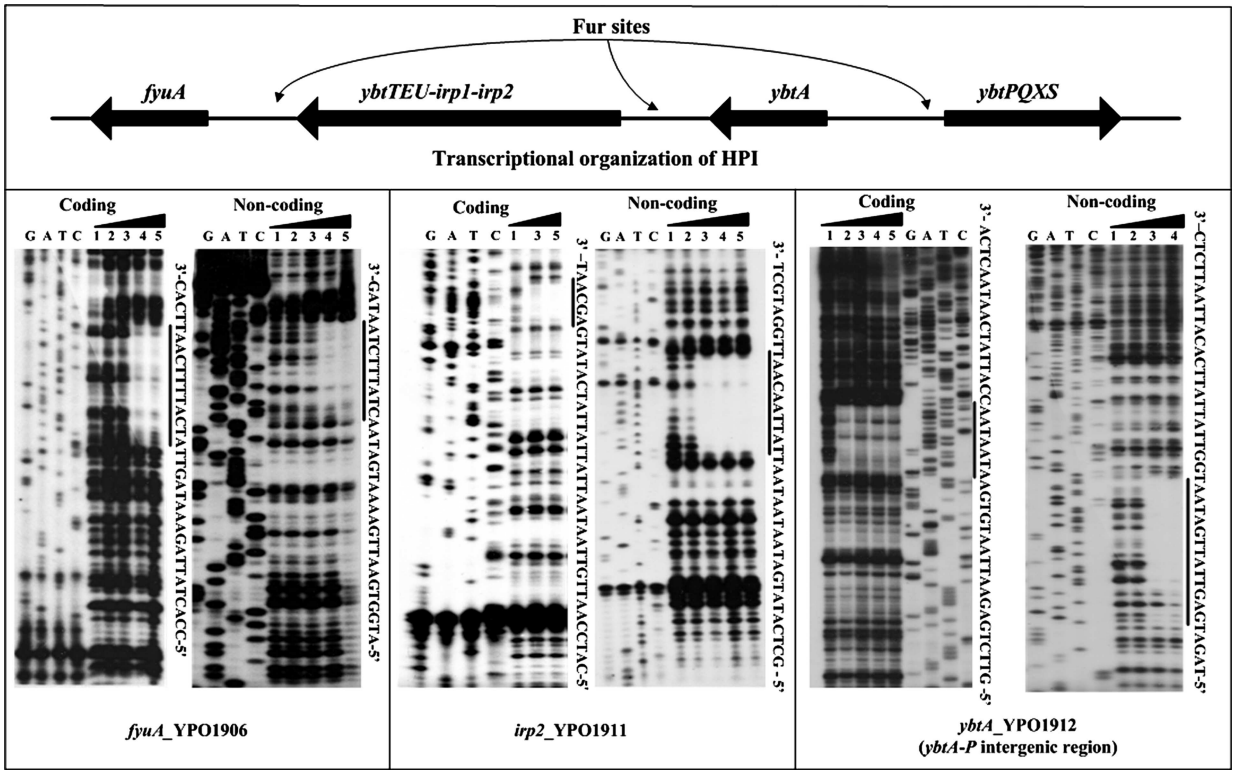

FIG. 4. DNase I footprinting assays. Coding and noncoding strands containing the predicted Fur box region were labeled with [γ-^{32}P] at the 5′ end, incubated with various amounts of purified His-Fur (lanes 1, 2, 3, 4, and 5 contained 0, 500, 1,000, 2,000, and 3,000 nM, respectively), and subjected to DNase I footprinting assays. Lanes G, A, T, and C represent the Sanger sequence reactions. On the right-hand side is indicated the protected region (bold line). The DNA sequences of footprints are shown from the bottom (5′) to the top (3′).

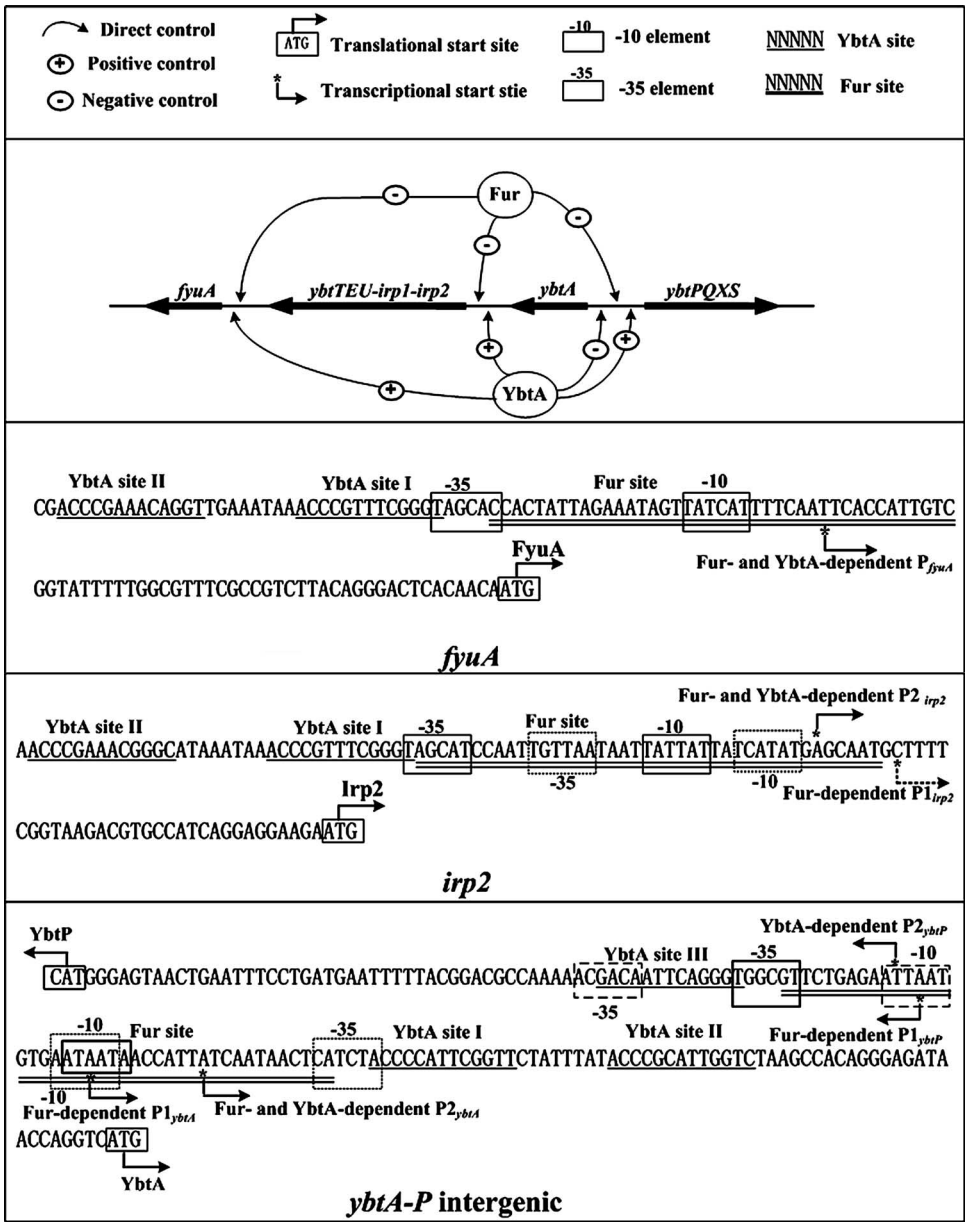

FIG. 5. Transcriptional organization of the Ybt locus under the control of Fur and YbtA. Shown is the Fur/YbtA regulatory network consisting of the Fur and YbtA regulator plus the four operons of HPI. Transcription and/or translational start sites, core promoter region (−10 and −35 elements), and Fur/YbtA sites are depicted for each promoter to give a map of Fur/YbtA-DNA interactions within the HPI.

For each promoter DNA tested, His-Fur protected a single distinct region against the DNase I digestion in a dose-dependent fashion (Fig. 4). Each footprint harbored a sequence resembling the predicted *Y. pestis* Fur box. These footprint regions were considered the Fur sites (Fig. 4).

The Fur/YbtA regulatory network: a map of regulator-DNA interactions within HPI. In the present study, we confirmed that the Fur protein repressed the whole *ybt* locus in response to excess extracellular iron and then defined the Fur sites within the *ybt* locus by using DNase I footprinting. In addition, the primer extension assay was used to determine the transcriptional start sites of Fur-dependent promoters and to help to localize the promoter −10 and −35 elements.

In addition to the Fur protein, the YbtA has been shown to be another transcriptional regulator that functions as an activator of *irp2-irp1-ybtUTE*, *ybtPQXS*, and *fyuA* and as a repressor of its own transcription (3, 14). The YbtA-DNA interactions within the HPI in *Y. pestis* have been elucidated recently (3).

Taking all of the above results together, we depicted the organization of Fur- and YbtA-dependent promoters to construct a prototype Fur/YbtA regulatory network (Fig. 5). Fur and YbtA shared all of the four operons within the HPI as the direct targets at the transcriptional level. All of the Fur- and/or YbtA-dependent promoters were elucidated according to the primer extension assay. For *fyuA*, there was only a single pro-

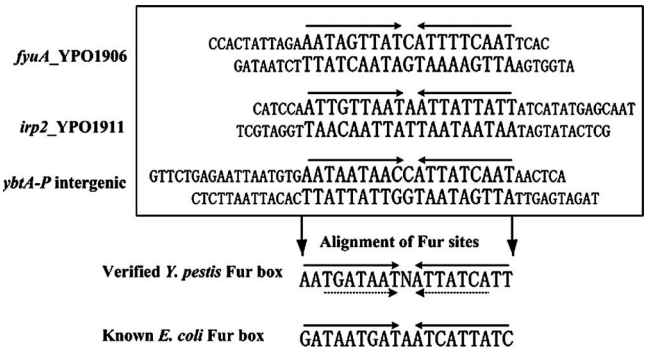

FIG. 6. Alignment of Fur sites to generate the Fur box. The footprint regions (Fur sites) determined by the DNase I footprinting assays were aligned to generate the Fur box. The 9-1-9 and 7-1-7 direct repeat elements were indicated by solid and dashed arrows, respectively.

moter (P_{fyuA}) that was shared by Fur and YbtA, while *irp2-irp1-ybtUTE*, *ybtA*, and *ybtPQXS* had two promoters. All of the promoters of *irp2-irp1-ybtUTE* ($P1_{irp2}$ and $P2_{irp2}$) and *ybtA* ($P1_{ybtA}$ and $P2_{ybtA}$) were recognized by Fur. For the two promoters of the *ybtPQXS* operon, one ($P1_{ybtP}$) was under the control of Fur, while the other one ($P2_{ybtP}$) was regulated by YbtA.

Figure 5 also gave a physical map of Fur- and YbtA-DNA interactions within the HPI. The Fur regulator recognized a single DNA site in each promoter region, while it seemed that YbtA was able to bind to at least two relatively shorter sites. No overlapping of Fur and Ybt sites within a specific promoter region was observed. *ybtA* and *ybtPQXS* were divergently transcribed. A single Fur-protected region in each of the coding and noncoding strands of the *ybtA/ybtP* intergenic region was identified. Thus, these two genes shared a single Fur site to mediate their transcriptional regulation. There were three YbtA sites disclosed in the *ybtA/ybtP* intergenic region, and both *ybtA* and *ybtPQXS* had a single YbtA-dependent promoter. By deleting the three YbtA sites systematically and by using the *ybtA* and *ybtP* transcriptional fusions, it has been determined that different modes of YbtA binding are responsible for the activation of *ybtPQXS* and the repression of *ybtA* in *Y. enterocolitica*, and a model of *ybtP* and *ybtA* promoter regulation has been established accordingly (2). Given the high conservation of HPI in the *Yersinia* spp., the mechanisms described above of transcriptional regulation by YbtA should generally be shared by *Y. pestis*.

Verified *Y. pestis* Fur box. As described above, by using the bioinformatics tools, we predicted the *Y. pestis* Fur box sequence that was an overrepresented motif in the promoter regions of the iron-Fur modulon members (35). Here, the above footprint regions were aligned to graphically describe the presence of a 9-1-9 direct repeat element in each of them. As shown in Fig. 6, the resulting Fur box confirmed the one disclosed by the previous computational promoter analysis (35). This verified *Y. pestis* Fur box showed six position differences compared to the *E. coli* Fur box.

Although previous studies on the *E. coli* Fur box have introduced the notion that Fur recognizes two 9-bp inverted repeats, 5′-GATAATGAT-3′, separated by one unmatched nucleotide, subsequent reports have strongly indicated that, for various bacteria (e.g., *E. coli*, *Bacillus subtilis*, and *Pseudomonas aeruginosa*), the primary DNA determinants for Fur recognition include a core 7-1-7 (or closely related) inverted repeat of TGATAATNATTATCA (1, 4, 5, 13, 24). This 7-1-7 inverted repeat is also found in the *Y. pestis* Fur box.

Concluding remarks. Based on a former microarray analysis, together with a former prediction of Fur box, a total of 32 putative operons in *Y. pestis* were shown by RT-PCR and primer extension analysis to be regulated by Fur. As determined by EMSA, the purified His-Fur was able to bind to the promoter DNA regions of all of these operons. Although Fur bound to the promoters of *fcuA* and *fepB*, no iron-Fur dependent regulation of them was observed. The detection of Fur-independent *fcuA* and *fepB* expression is confined to strain 201 under the growth conditions described here. These two genes were still presumed to be under the direct control of Fur, since Fur recognized their promoters and both of them encoded the iron acquisition functions. Accordingly, the 34 putative operons described here, including *fcuA* and *fepB*, were assigned to the Fur regulon of *Y. pestis* (here, the regulon was defined as the collection of direct targets of a specific transcriptional regulator). Thus, the *Y. pestis* Fur is a global regulator (both an activator and a repressor) that directly controls not only almost all of the iron assimilation functions but also a variety of genes involved in various non-iron functions for governing a complex regulatory cascade in *Y. pestis*.

We searched the CO92 genome for sites matching the PFM in supplemental data S1, generating a weight score for the promoter DNA of each gene in the genome. When a score value of 10 was taken as the cutoff value, more than 70 genes were picked out as the potential direct Fur targets. This in silico analysis indicates that there are still some other direct Fur targets to be identified. Among them is especially the *ryhB* gene that encodes a small RNA responsible for regulating bacterial iron-assimilation genes. The identification of additional direct Fur targets in *Y. pestis* is under way.

ACKNOWLEDGMENTS

We thank Xinming Song of the Veterinary Infectious Disease Organization, Saskatoon, Saskatchewan, Canada, for careful reading and revision of the manuscript.

Financial support for this study came from the National Natural Science Foundation of China for Distinguished Young Scholars (no. 30525025). All of the experiments in the present study were completed in R. Yang's laboratory.

REFERENCES

1. **Andrews, L. S., S. DeBlanc, C. D. Veal, and D. L. Park.** 2003. Response of *Vibrio parahaemolyticus* O3:K6 to a hot water/cold shock pasteurization process. Food Addit. Contam. **20:**331–334.
2. **Anisimov, R., D. Brem, J. Heesemann, and A. Rakin.** 2005. Molecular mechanism of YbtA-mediated transcriptional regulation of divergent overlapping promoters *ybtA* and *irp6* of *Yersinia enterocolitica*. FEMS Microbiol. Lett. **250:**27–32.
3. **Anisimov, R., D. Brem, J. Heesemann, and A. Rakin.** 2005. Transcriptional regulation of high pathogenicity island iron uptake genes by YbtA. Int. J. Med. Microbiol. **295:**19–28.
4. **Baichoo, N., and J. D. Helmann.** 2002. Recognition of DNA by Fur: a reinterpretation of the Fur box consensus sequence. J. Bacteriol. **184:**5826–5832.
5. **Baichoo, N., T. Wang, R. Ye, and J. D. Helmann.** 2002. Global analysis of the *Bacillus subtilis* Fur regulon and the iron starvation stimulon. Mol. Microbiol. **45:**1613–1629.
6. **Bearden, S. W., and R. D. Perry.** 1999. The Yfe system of *Yersinia pestis* transports iron and manganese and is required for full virulence of plague. Mol. Microbiol. **32:**403–414.

7. **Bearden, S. W., T. M. Staggs, and R. D. Perry.** 1998. An ABC transporter system of *Yersinia pestis* allows utilization of chelated iron by *Escherichia coli* SAB11. J. Bacteriol. **180:**1135–1147.
8. **Buchrieser, C., C. Rusniok, L. Frangeul, E. Couve, A. Billault, F. Kunst, E. Carniel, and P. Glaser.** 1999. The 102-kilobase *pgm* locus of *Yersinia pestis*: sequence analysis and comparison of selected regions among different *Yersinia pestis* and *Yersinia pseudotuberculosis* strains. Infect. Immun. **67:**4851–4861.
9. **Carniel, E.** 1999. The *Yersinia* high-pathogenicity island. Int. Microbiol. **2:**161–167.
10. **Carniel, E.** 2001. The *Yersinia* high-pathogenicity island: an iron-uptake island. Microbes Infect. **3:**561–569.
11. **Datsenko, K. A., and B. L. Wanner.** 2000. One-step inactivation of chromosomal genes in *Escherichia coli* K-12 using PCR products. Proc. Natl. Acad. Sci. USA **97:**6640–6645.
12. **Delany, I., R. Rappuoli, and V. Scarlato.** 2004. Fur functions as an activator and as a repressor of putative virulence genes in *Neisseria meningitidis*. Mol. Microbiol. **52:**1081–1090.
13. **Escolar, L., J. Perez-Martin, and V. de Lorenzo.** 1999. Opening the iron box: transcriptional metalloregulation by the Fur protein. J. Bacteriol. **181:**6223–6229.
14. **Fetherston, J. D., S. W. Bearden, and R. D. Perry.** 1996. YbtA, an AraC-type regulator of the *Yersinia pestis* pesticin/yersiniabactin receptor. Mol. Microbiol. **22:**315–325.
15. **Forman, S., M. J. Nagiec, J. Abney, R. D. Perry, and J. D. Fetherston.** 2007. Analysis of the aerobactin and ferric hydroxamate uptake systems of *Yersinia pestis*. Microbiology **153:**2332–2341.
16. **Gong, S., S. W. Bearden, V. A. Geoffroy, J. D. Fetherston, and R. D. Perry.** 2001. Characterization of the *Yersinia pestis* Yfu ABC inorganic iron transport system. Infect. Immun. **69:**2829–2837.
17. **Han, Y., J. Qiu, Z. Guo, H. Gao, Y. Song, D. Zhou, and R. Yang.** 2007. Comparative transcriptomics in *Yersinia pestis*: a global view of environmental modulation of gene expression. BMC Microbiol. **7:**96.
18. **Hantke, K.** 2001. Iron and metal regulation in bacteria. Curr. Opin. Microbiol. **4:**172–177.
19. **Heath, D. G., G. W. Anderson, Jr., J. M. Mauro, S. L. Welkos, G. P. Andrews, J. Adamovicz, and A. M. Friedlander.** 1998. Protection against experimental bubonic and pneumonic plague by a recombinant capsular F1-V antigen fusion protein vaccine. Vaccine **16:**1131–1137.
20. **Kirillina, O., A. G. Bobrov, J. D. Fetherston, and R. D. Perry.** 2006. Hierarchy of iron uptake systems: Yfu and Yiu are functional in *Yersinia pestis*. Infect. Immun. **74:**6171–6178.
21. **Kothapalli, R., S. J. Yoder, S. Mane, and T. P. Loughran, Jr.** 2002. Microarray results: how accurate are they? BMC Bioinform. **3:**22.
22. **Pace, J. L., T. J. Chai, H. A. Rossi, and X. Jiang.** 1997. Effect of bile on *Vibrio parahaemolyticus*. Appl. Environ. Microbiol. **63:**2372–2377.
23. **Perry, R. D., and J. D. Fetherston.** 1997. *Yersinia pestis*: etiologic agent of plague. Clin. Microbiol. Rev. **10:**35–66.
24. **Pohlmann, A., R. Cramm, K. Schmelz, and B. Friedrich.** 2000. A novel NO-responding regulator controls the reduction of nitric oxide in *Ralstonia eutropha*. Mol. Microbiol. **38:**626–638.
25. **Schubert, S.** 2004. The *Yersinia* high-pathogenicity island (HPI): evolutionary and functional aspects. Int. J. Med. Microbiol. **294:**83–94.
26. **Schuchhardt, J., D. Beule, A. Malik, E. Wolski, H. Eickhoff, H. Lehrach, and H. Herzel.** 2000. Normalization strategies for cDNA microarrays. Nucleic Acids Res. **28:**E47.
27. **Sebaihia, M., S. D. Bentley, M. T. Holden, and J. Parkhill.** 2003. The good, the bad and the ugly? Trends Microbiol. **11:**204–205.
28. **Song, Y., Z. Tong, J. Wang, L. Wang, Z. Guo, Y. Han, J. Zhang, D. Pei, D. Zhou, H. Qin, X. Pang, J. Zhai, M. Li, B. Cui, Z. Qi, L. Jin, R. Dai, F. Chen, S. Li, C. Ye, Z. Du, W. Lin, J. Yu, H. Yang, P. Huang, and R. Yang.** 2004. Complete genome sequence of *Yersinia pestis* strain 91001, an isolate avirulent to humans. DNA Res. **11:**179–197.
29. **Straley, S. C., and W. S. Bowmer.** 1986. Virulence genes regulated at the transcriptional level by Ca^{2+} in *Yersinia pestis* include structural genes for outer membrane proteins. Infect. Immun. **51:**445–454.
30. **Thompson, J. M., H. A. Jones, and R. D. Perry.** 1999. Molecular characterization of the hemin uptake locus (*hmu*) from *Yersinia pestis* and analysis of *hmu* mutants for hemin and hemoprotein utilization. Infect. Immun. **67:**3879–3892.
31. **van Helden, J.** 2003. Regulatory sequence analysis tools. Nucleic Acids Res. **31:**3593–3596.
32. **Wandersman, C., and P. Delepelaire.** 2004. Bacterial iron sources: from siderophores to hemophores. Annu. Rev. Microbiol. **58:**611–647.
33. **Yin, Z. X., J. G. He, W. X. Deng, and S. M. Chan.** 2003. Molecular cloning, expression of orange-spotted grouper goose-type lysozyme cDNA, and lytic activity of its recombinant protein. Dis. Aquat. Organ. **55:**117–123.
34. **Zhou, D., Y. Han, and R. Yang.** 2006. Molecular and physiological insights into plague transmission, virulence and etiology. Microbes Infect. **8:**273–284.
35. **Zhou, D., L. Qin, Y. Han, J. Qiu, Z. Chen, B. Li, Y. Song, J. Wang, Z. Guo, J. Zhai, Z. Du, X. Wang, and R. Yang.** 2006. Global analysis of iron assimilation and fur regulation in *Yersinia pestis*. FEMS Microbiol. Lett. **258:**9–17.
36. **Zhou, D., Z. Tong, Y. Song, Y. Han, D. Pei, X. Pang, J. Zhai, M. Li, B. Cui, Z. Qi, L. Jin, R. Dai, Z. Du, J. Wang, Z. Guo, P. Huang, and R. Yang.** 2004. Genetics of metabolic variations between *Yersinia pestis* biovars and the proposal of a new biovar, microtus. J. Bacteriol. **186:**5147–5152.
37. **Zhou, D., and R. Yang.** 2006. Global analysis of gene transcription regulation in prokaryotes. Cell Mol. Life Sci. **63:**2260–2290.